

# Implementation of superconductor/ferromagnet/superconductor $\pi$ -shifters in superconducting digital and quantum circuits

A. K. Feofanov<sup>1</sup>, V. A. Oboznov<sup>2</sup>, V. V. Bol'ginov<sup>2</sup>, J. Lisenfeld<sup>1</sup>, S. Poletto<sup>1</sup>, V. V. Ryazanov<sup>2</sup>, A. N. Rossolenko<sup>2</sup>, M. Khabipov<sup>3</sup>, D. Balashov<sup>3</sup>, A. B. Zorin<sup>3</sup>, P. N. Dmitriev<sup>4</sup>, V. P. Koshelets<sup>4</sup> and A. V. Ustinov<sup>1\*</sup>

**High operation speed and low energy consumption may allow the superconducting digital single-flux-quantum circuits to outperform traditional complementary metal-oxide-semiconductor logic. The remaining major obstacle towards high element densities on-chip is a relatively large cell size necessary to hold a magnetic flux quantum  $\Phi_0$ . Inserting a  $\pi$ -type Josephson junction<sup>1,2</sup> in the cell is equivalent to applying flux  $\Phi_0/2$  and thus makes it possible to solve this problem<sup>3</sup>. Moreover, using  $\pi$ -junctions in superconducting qubits may help to protect them from noise<sup>4,5</sup>. Here we demonstrate the operation of three superconducting circuits—two of them are classical and one quantum—that all utilize such  $\pi$ -phase shifters realized using superconductor/ferromagnet/superconductor sandwich technology<sup>6</sup>. The classical circuits are based on single-flux-quantum cells, which are shown to be scalable and compatible with conventional niobium-based superconducting electronics. The quantum circuit is a  $\pi$ -biased phase qubit, for which we observe coherent Rabi oscillations. We find no degradation of the measured coherence time compared to that of a reference qubit without a  $\pi$ -junction.**

In superconducting circuits, currents can flow without applying any electric field. The role of the electrostatic potential difference required to drive a current in conventional circuits is played here by a difference  $\varphi$  between the phases of the superconducting order parameters. In the absence of current,  $\varphi$  is zero, but this can be altered by inserting a particular type of superconducting weak link, a so-called  $\pi$ -junction<sup>1,2</sup>, yielding a phase shift of  $\pi$ . The fundamental property of superconducting weak links is a  $2\pi$ -periodic current–phase relation. The supercurrent through a conventional Josephson junction is usually described by the harmonic relation  $I_s = I_C \sin\varphi$ , where  $I_C$  is the critical current, whereas the  $\pi$ -junction has the inverse current–phase relation  $I_s = I_C \sin(\varphi + \pi) = -I_C \sin\varphi$ . The  $\pi$ -junctions were theoretically proposed about three decades ago, whereas their remarkable properties have been demonstrated in experiments notably later<sup>6–8</sup>. Practical implementations of  $\pi$ -junctions have been widely discussed for a variety of different technologies. These include approaches using superconductors with  $d$ -wave order parameter symmetry<sup>7,9,10</sup>, circuits with non-equilibrium current injection<sup>8</sup>, junctions with ferromagnetic layers<sup>6</sup> and junctions with gated carbon nanotubes<sup>11</sup>.

The ideas of using  $\pi$ -junctions in superconducting classical and quantum circuits have been explored in several theoretical proposals. In classical digital logic, a complementary Josephson junction inverter<sup>12</sup> was suggested as a superconducting analogue of the complementary metal–oxide–semiconductor logic. It relies on using superconducting quantum interference devices (SQUIDs) of conventional (0-junctions) and  $\pi$ -types and requires that 0- and  $\pi$ -junctions have similar  $I_C$  and normal-state resistance. These technologically stringent requirements can be softened by using an alternative ‘asymmetric’ approach<sup>3</sup> that employs  $\pi$ -junctions as passive phase shifters (phase inverters) in basic cells of the modified single-flux-quantum (SFQ) logic. Here the  $\pi$ -junction critical current  $I_C$  is chosen to be much larger than that of conventional 0-junctions employed in the very same SFQ cell, so the phase difference across the  $\pi$ -junction is always close to  $\pi$  even at zero magnetic field. As the total change of the order parameter’s phase over the closed path must become a multiple of  $2\pi$ , the ‘missing’ phase difference of  $\pi$  or  $-\pi$  is induced on the remaining part of the cell by a spontaneously generated superconducting current.

The first proposal for using a loop with an integrated  $\pi$ -junction as a superconducting quantum circuit<sup>4,5</sup> featured a superposition of two persistent current states in a loop at zero magnetic field, in analogy to a spin-1/2 system. The  $\pi$ -junctions required here must have very low dissipation (high normal resistance), which so far has seemed unattainable for any of the existing technologies for making  $\pi$ -junctions. The alternative usage of  $\pi$ -junctions as passive phase shifters offers an advantage for the operation of superconducting flux qubits at the degeneracy point requiring zero or a very small external magnetic field. Potentially, this allows noise and electromagnetic interference induced by magnetic field sources to be minimized. There remains an open question: do  $\pi$ -junctions themselves introduce any intrinsic decoherence when they are inserted into a superconducting quantum circuit?

The origin of the  $\pi$ -state in a superconductor/ferromagnet/superconductor (SFS) junction is an oscillating and sign-reversing superconducting order parameter in the ferromagnet close to the superconductor/ferromagnet interface<sup>2,13</sup>. Owing to these oscillations, different signs of the order parameter can occur at the two banks of the SFS sandwich when the ferromagnetic layer thickness is of the order of half an oscillation period, which corresponds to a sign change of the supercurrent and

<sup>1</sup>Physikalisches Institut and DFG Center for Functional Nanostructures (CFN), Karlsruhe Institute of Technology, Wolfgang-Gaede-Str.1, D-76131 Karlsruhe, Germany, <sup>2</sup>Institute of Solid State Physics, Russian Academy of Science, Chernogolovka 142432, Russia, <sup>3</sup>Physikalisch-Technische Bundesanstalt, Bundesallee 100, 38116 Braunschweig, Germany, <sup>4</sup>Kotel'nikov Institute of Radio Engineering and Electronics, Russian Academy of Science, Mokhovaya 11, Building 7, Moscow 125009, Russia. \*e-mail: ustinov@kit.edu.

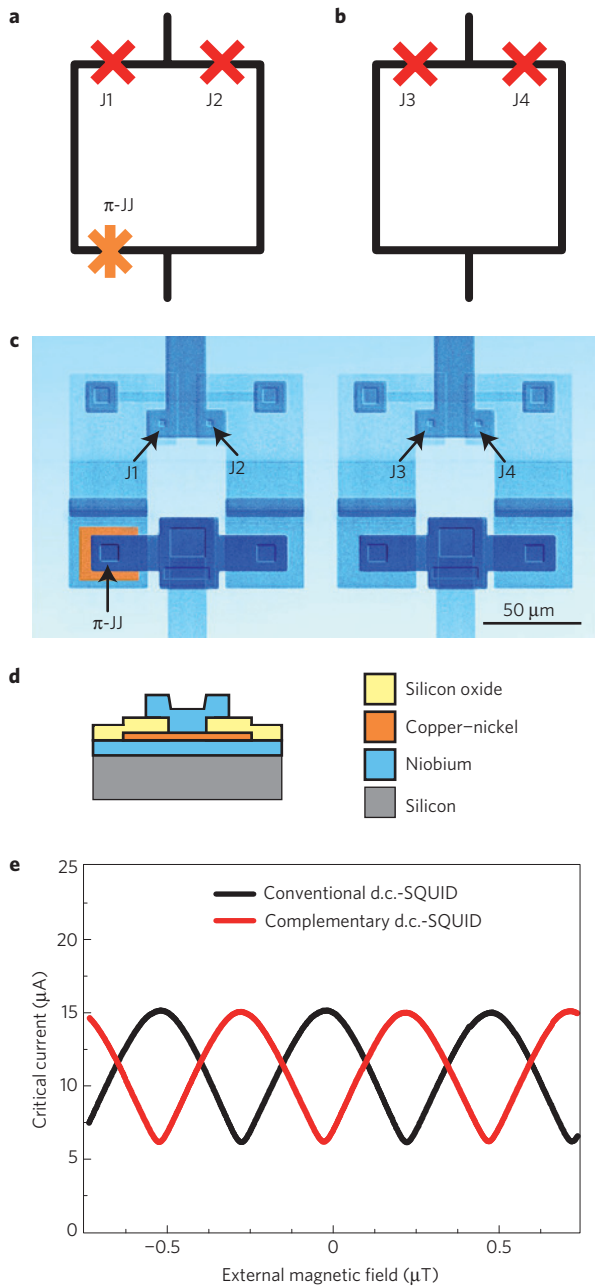


**Figure 1 | Complementary d.c.-SQUIDs.** **a**, Schematic of a complementary d.c.-SQUID employing two conventional Josephson junctions (red crosses) and a  $\pi$ -junction (orange star). **b**, Schematic of a conventional d.c.-SQUID used as a reference device. **c**, A scanning electron micrograph of the fabricated d.c.-SQUIDs. The ferromagnetic layer is shown in orange. **d**, Schematic cross-section through an SFS  $\pi$ -junction. **e**, Dependencies of the critical currents of the devices shown in **c** versus the applied magnetic field. The red curve related to the  $\pi$ -SQUID is shifted by half a period. The modulation amplitude is limited, as the factor  $2LI_C \approx 0.85 \Phi_0$ .

a negative Josephson coupling energy. This behaviour was first observed experimentally on Nb/CuNi/Nb sandwiches in ref. 6. Further experiments reported the spontaneous flux<sup>14</sup> and half-periodical shifts of the superconducting interferometer  $I_C(H)$  dependence<sup>15</sup> as well as a sign change of the junction current–phase relation<sup>16</sup>. Recently, the critical current density of the Nb/Cu<sub>0.47</sub>Ni<sub>0.53</sub>/Nb  $\pi$ -junctions was pushed above  $1,000 \text{ A cm}^{-2}$  (ref. 17). These junctions are compatible with conventional niobium thin-film technology and thus can be

easily integrated in the conventional fabrication process of superconducting digital circuits.

To verify the operation of  $\pi$ -junction phase shifters in an analogue regime, we fabricated two geometrically identical superconducting loops (see schematic in Fig. 1a,b) on a single Si substrate (see Fig. 1c). The circuit Fig. 1b is a two-junction interferometer conventionally called a d.c.-SQUID. The configuration of the circuit in Fig. 1a is nominally identical to that in Fig. 1b, except that an SFS  $\pi$ -junction has been inserted in the left branch of the loop, seen in the lower left corner of the circuit image in Fig. 1c. The on-chip distance between the centres of the two loops is  $140 \mu\text{m}$ , so both interferometers are exposed to the same magnetic field during the experiment. The  $\pi$ -junction critical current is much larger than those of the tunnel junctions. Therefore, during the dynamic switchings in the rest of the circuit,  $\pi$ -junctions do not introduce any noticeable phase shifts deviating from  $\pi$ .

The dependencies of the critical currents  $I_C(H)$  of the two devices shown in Fig. 1a,b are presented in Fig. 1e. Whereas both curves have the same shape, they are shifted by a half-period. A small offset of the symmetry axes for both curves from the zero-field value is due to a small residual magnetic field in the cryostat. The minimum of the red  $I_C(H)$  curve at zero field is due to inclusion of the  $\pi$ -junction in the superconducting loop. In the conventional SQUID, the same frustrated state exists at an external magnetic field corresponding to half-integer numbers of magnetic flux quanta per cell. Thus, embedding an SFS  $\pi$ -phase shifter into a superconducting loop indeed leads to self-biasing of the loop by a spontaneously induced supercurrent.

In the second experiment, we demonstrate the functionality of the  $\pi$ -phase shifter included in a superconducting logic circuit. The SFQ logic circuits enable processing of information in the form of single flux quanta that can be stored in elementary superconducting cells including inductors and Josephson junctions. Dynamically, this information is represented by SFQ voltage pulses<sup>18</sup> having a quantized area  $\int V(t) dt = \Phi_0$  and corresponding to the transfer of one flux quantum across a Josephson junction. The first SFQ circuits with active  $\pi$ -elements were made of high- $T_C$  superconductor (YBa<sub>2</sub>Cu<sub>3</sub>O<sub>7- $\delta$</sub> ) employing  $d$ -wave pairing symmetry combined with conventional low- $T_C$  superconductor (Nb; ref. 19). Operation of the circuits with the phase shifting element based on frozen flux quanta<sup>20</sup> has been tested earlier in ref. 21. Here we present the first demonstration of the functionality of an SFS  $\pi$ -phase shifter integrated in a conventional Nb SFQ circuit. Figure 2 shows the layout and operation of our test SFQ circuit, represented by a two-stage frequency divider.

Another attractive application of SFS  $\pi$ -junctions is their use as phase shifters in coherent quantum circuits realizing superconducting quantum bits. The answer to the question of whether or not  $\pi$ -junctions can become useful in superconducting circuits designed for quantum computing applications depends on their impact on the coherence properties of the qubits. Potential sources of decoherence introduced by  $\pi$ -junctions can for instance be spin-flips in the ferromagnetic barrier<sup>22</sup>, either occurring randomly or being driven by high-frequency currents and fields, as well as the dynamic response of the magnetic domain structure<sup>23</sup>. We address these important coherence issues in a third experiment reported in this letter, in which we use an SFS  $\pi$ -junction to self-bias a superconducting phase qubit. We have chosen here a phase qubit<sup>24</sup> rather than a flux qubit<sup>25</sup> because of the simpler fabrication procedure for the former. The results reported below would nevertheless remain fully applicable to flux qubits.

A phase qubit<sup>24</sup> consists of a single Josephson junction embedded in a superconducting loop. It is magnetically biased close to an integer number of flux quanta in the loop. At such a bias, the potential energy of the qubit exhibits an asymmetric double-well potential, whereas two quantized energy eigenvalues of

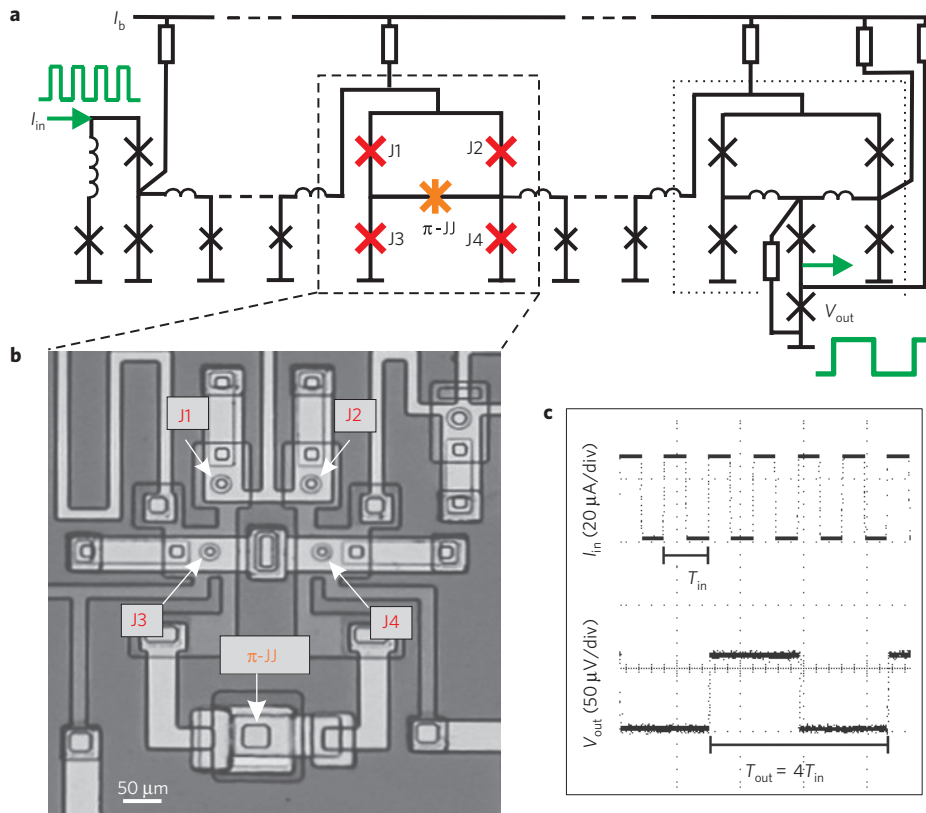


**Figure 2 |  $\pi$ -SFQ two-stage frequency divider.** **a**, Schematic of the frequency binary divider. This two-stage circuit includes the TFF with an SFS  $\pi$ -junction (inside the dashed-line square) and conventional TFF (inside dotted-line square), with Josephson transmission lines enabling delivery of SFQ pulses to the inputs of TFFs. **b**, Micrograph of the TFF with a  $\pi$ -junction. **c**, Oscilloscope output verifying correct operation of this SFQ circuit, that is, division of the frequency of input pulses by four.

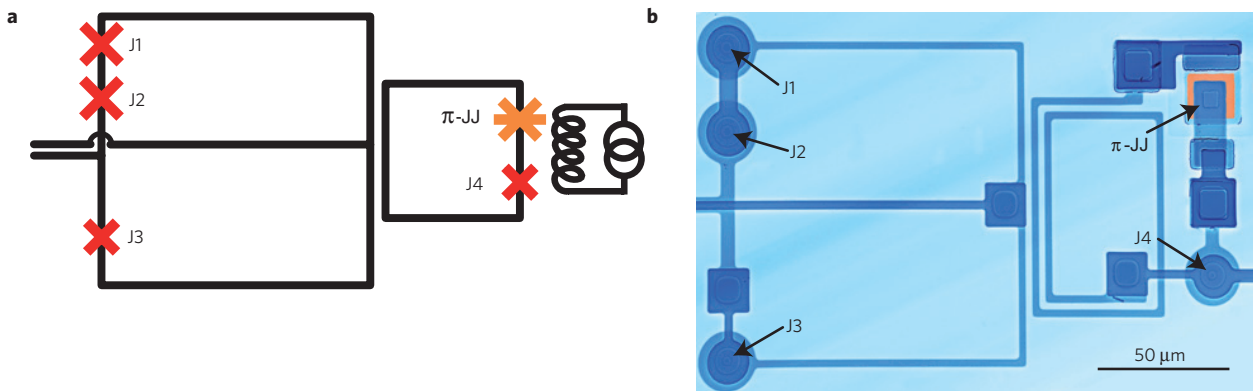


**Figure 3 | Self-biased phase qubit.** **a**, Schematic of a phase qubit circuit used to test the decoherence properties of the  $\pi$ -junction. The qubit is realized by the central loop with embedded conventional and  $\pi$ -Josephson junctions. The larger loop to its left is a d.c.-SQUID for qubit readout. To the right of the qubit is a weakly coupled flux bias coil. **b**, Scanning electron microscope picture of the realized phase qubit employing a  $\pi$ -junction in the qubit loop. The flux bias coil is not shown.

the phase localized inside the shallow well are used as the logical qubit states  $|0\rangle$  and  $|1\rangle$ . Figure 3a shows a circuit schematic and Fig. 3b a micrograph of the tested sample. Here, a  $\pi$ -junction is connected in series to the phase qubit's tunnel junction. Coherent qubit operation is demonstrated by the data reported in Fig. 4a, showing Rabi oscillation of the excited qubit state population probability as a function of the duration of a resonant microwave pulse. The oscillations exhibit a decay time of about 4 ns, which is a typical value reachable in samples fabricated using similar fabrication processes<sup>26</sup>. To find out whether the  $\pi$ -junction does introduce extra decoherence, a conventional phase qubit without

a  $\pi$ -junction was fabricated on the same wafer. As shown in Fig. 4b, this reference qubit shows a nearly identical decay time for Rabi oscillations.

Thus, we obtained experimentally that the decay time limited by the  $\pi$ -junction is significantly larger than 4 ns. We compared the measured decoherence time with the theoretical predictions<sup>27</sup>. We assume here an overdamped SFS  $\pi$ -junction having a normal resistance of  $R_{N,\pi} \approx 500 \mu\Omega$  and a critical current  $I_{C,\pi} \approx 50 \mu\text{A}$ . In our case, the qubit level splitting  $\Delta \gg 2eI_{C,\pi}R_{N,\pi}$ , where  $\Delta \approx h \cdot 13.5 \text{ GHz}$ ,  $h$  is Planck's constant and  $e$  is the elementary charge. Here, the energy  $2eI_{C,\pi}R_{N,\pi} \approx h \cdot 12 \text{ MHz}$  is associated

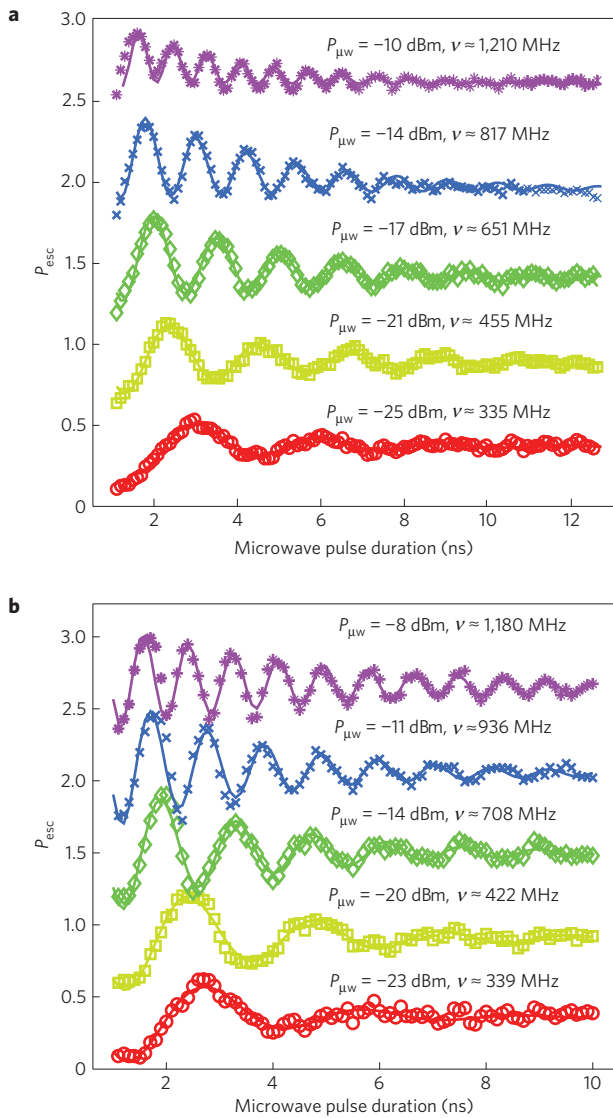


**Figure 4 | Rabi oscillations between the ground and the excited qubit states resulted from resonant microwave driving.** **a, b**, Rabi oscillations observed in the phase qubit with an embedded  $\pi$ -junction (**a**) and a conventional phase qubit made on the same wafer as a reference (**b**). Each data set was taken using the indicated microwave power as delivered by the generator, giving rise to a change in the coherent oscillation frequency as expected for Rabi oscillation.

with the characteristic Josephson frequency of our SFS  $\pi$ -junction. Simplifying the expression for the relaxation time<sup>27</sup> in this limit (see Supplementary Information), we can theoretically estimate the relaxation time  $\tau_{\text{relax}}$  as

$$\tau_{\text{relax}} \approx \frac{\Delta}{2I_C^2 R_{N,\pi}} \approx 2 \text{ ns} \quad (1)$$

Here,  $I_C \approx 2 \mu\text{A}$  is the critical current of the small SIS qubit junction. The estimated value of the energy relaxation time is of the same order as the measured decoherence time of our reference qubit without an SFS  $\pi$ -junction. In fact, the theoretical estimate is valid for the qubit operated as a flux qubit. In the phase qubit regime, the relaxation time is expected to be longer because the amplitude of the microwave current in the qubit loop is much smaller than  $I_C$ , allowing us to conclude that at least on the observable timescale no extra decoherence is introduced by the SFS  $\pi$ -phase shifter

employed in this circuit and that the decoherence in both qubits is limited by some other mechanism. We note, however, that the expected relaxation time equation (1) can be enhanced by using SFS junctions having a smaller resistance  $R_{N,\pi}$ .

In contrast to  $\pi$ -junctions based on high- $T_C$  superconductor junctions with  $d$ -wave pairing symmetry, SFS elements can have a sufficiently large critical current, so that the desired  $\pi$ -phase shift remains reliably fixed during circuit operation. In distinction from phase-shifting loops with a frozen magnetic flux<sup>20</sup>, the SFS circuits are much more compact and do not require trapping a well-defined integer number flux quanta in their superconducting loops.

As an outlook, a significant reduction in the size of the demonstrated SFS  $\pi$ -phase shifters for digital circuits is readily possible, opening the way to scaling superconducting logic circuits down to submicrometre dimensions<sup>3</sup>. The visualization of the magnetic structure of our ferromagnetic layer material shows domain sizes smaller than 100 nm. Therefore, we believe that a reduction of the junction planar dimensions down to 300–500 nm is feasible. Furthermore, combining the high- $j_C$   $\pi$ -junction technology with *in-situ*-grown tunnel barriers<sup>28,29</sup> may open the way towards active inverter elements that are in great demand for superconducting electronics.

## Methods

**Samples.** Details on the fabrication technique for tunnel Nb/Al/AIO<sub>x</sub>/Nb junctions employed in complementary SQUID circuits are presented in ref. 30. In brief, a three-layer Nb/Al/AIO<sub>x</sub>/Nb structure is deposited by magnetron sputtering. The layers have thicknesses of 180, 7 and 80 nm, respectively. Aluminium is oxidized in pure oxygen to form a tunnel barrier having a critical current density of about 200 A cm<sup>-2</sup>. The junction area, here 10  $\mu\text{m}^2$ , is defined by reactive ion etching and subsequent SiO<sub>2</sub> deposition. Resistive shunts in parallel to the tunnel junctions are formed by a molybdenum layer with a specific resistance of 2  $\Omega$  per square.

For fabrication of SFS  $\pi$ -junctions, the bottom Nb electrode with a thickness of 110 nm was fabricated by d.c.-magnetron sputtering followed by a lift-off process. A 15-nm-thick Cu<sub>0.47</sub>Ni<sub>0.53</sub> layer (ferromagnetic layer) was deposited by radiofrequency sputtering after ion cleaning of the niobium surface. Afterwards, the insulating layer having a window that determines the junction area was prepared by the lift-off process. We used a 150-nm-thick SiO film as the insulator, which was thermally evaporated. The fabrication procedure was completed by Ar plasma cleaning and d.c.-magnetron sputtering of the upper niobium electrode of 240 nm thickness. A 10  $\times$  10  $\mu\text{m}^2$  junction normal resistance  $R_n$  is about 150  $\mu\Omega$ . The critical currents of such  $\pi$ -junctions are about 200  $\mu\text{A}$  and hence the junctions do not switch to the resistive state when embedded in loops with conventional tunnel junctions having critical currents of about 10  $\mu\text{A}$ . This large difference between two critical currents means that during the dynamic switchings in the rest of the circuit,  $\pi$ -junctions do not introduce any noticeable phase shifts deviating from  $\pi$ .

The qubit circuit was fabricated in a standard Nb/Al-AIO<sub>x</sub>/Nb trilayer process, whereas the  $\pi$ -junction was integrated subsequently by carrying out the further lithographic steps described above.

**$\pi$ -SFQ two-stage frequency divider dynamics.** The circuit is fed by current  $I_b$  through a network of resistors (top part of Fig. 2a), which provides current bias of individual Josephson junctions on the level of approximately 70% of their critical value  $I_C$ . The positive edges of rectangular trigger pulses ( $I_{\text{in}}$ ) are delivered to the first dividing stage of the circuit by means of a Josephson transmission line (left part of diagram in Fig. 2a) in the form of SFQ pulses. These pulses cause switching of this first stage of the circuit, the toggle flip-flop (TFF) with an integrated SFS  $\pi$ -phase shifter, which replaces a large inductance required in the conventional counterpart circuit for the realization of desired bistable behaviour. The output signal of the first TFF in the form of SFQ pulses is sent to the second dividing stage, which is realized as a conventional TFF circuit. The circuit output  $V_{\text{out}}$  time pattern shows a division of the frequency of the input pulses by four (with 19% margins for the main circuit parameters), which verifies its correct functioning.

**Phase qubit operation.** The qubit is controlled by inducing a small-amplitude microwave current in the loop. The current frequency is tuned in resonance to the  $|0\rangle$  to  $|1\rangle$  transition, giving rise to Rabi oscillation of the state population. Reading out the qubit is accomplished by applying a short d.c. flux pulse to the qubit loop, during which only the excited qubit state may tunnel to the neighbouring potential well. As this tunnelling event entails a flux quantum entering the qubit loop, reading out the qubit is concluded by a measurement of the flux threading the qubit loop by means of an inductively coupled d.c.-SQUID.

Received 30 October 2009; accepted 10 May 2010;  
published online 20 June 2010

## References

- Bulaevskii, L. N., Kuzii, V. V. & Sobyanin, A. A. Superconducting system with weak coupling to the current in the ground state. *J. Exp. Theor. Phys. Lett.* **25**, 290–294 (1977).
- Buzdin, A. I., Bulaevskij, L. N. & Panyukov, S. V. Critical-current oscillations as a function of the exchange field and thickness of the ferromagnetic metal (F) in an S–F–S Josephson junction. *J. Exp. Theor. Phys. Lett.* **35**, 178–180 (1982).
- Ustinov, A. V. & Kaplunenko, V. K. Rapid single-flux quantum logic using  $\pi$ -shifters. *J. Appl. Phys.* **94**, 5405–5407 (2003).
- Ioffe, L. B., Geshkenbein, V. B., Feigelman, M. V., Fauchère, A. L. & Blatter, G. Environmentally decoupled sds-wave Josephson junctions for quantum computing. *Nature* **398**, 679–681 (1999).
- Blatter, G., Geshkenbein, V. B. & Ioffe, L. B. Design aspects of superconducting-phase quantum bits. *Phys. Rev. B* **63**, 174511 (2001).
- Ryazanov, V. V. *et al.* Coupling of two superconductors through a ferromagnet: Evidence for a  $\pi$ -junction. *Phys. Rev. Lett.* **86**, 2427–2430 (2001).
- Van Harlingen, D. J. Phase-sensitive tests of the symmetry of the pairing state in the high-temperature superconductors—evidence for  $d_{x^2-y^2}$  symmetry. *Rev. Mod. Phys.* **67**, 515–535 (1995).
- Baselmans, J. J. A., Morpurgo, A. F., van Wees, B. & Klapwijk, T. M. Reversing the direction of supercurrent in a controllable Josephson junction. *Nature* **397**, 43–45 (1999).
- Testa, G. *et al.* Midgap state-based  $\pi$ -junctions for digital applications. *Appl. Phys. Lett.* **85**, 1202–1204 (2004).
- Hilgenkamp, H. *et al.* Ordering and manipulation of the magnetic moments in large-scale superconducting  $\pi$ -loop arrays. *Nature* **422**, 50–53 (2003).
- Cleuziou, J.-P., Wernsdorfer, W., Bouchiat, V., Ondarcuhu, T. & Monthieux, M. Carbon nanotube superconducting quantum interference device. *Nature Nanotech.* **1**, 53–59 (2006).
- Terzioglu, E. & Beasley, M. R. Complementary Josephson junction devices and circuits: A possible new approach to superconducting electronics. *IEEE Trans. Appl. Supercond.* **8**, 48–53 (1998).
- Buzdin, A. I. Proximity effects in superconductor–ferromagnet heterostructures. *Rev. Mod. Phys.* **77**, 935–976 (2005).
- Frolov, S. M. *et al.* Imaging spontaneous currents in superconducting arrays of  $\pi$ -junctions. *Nature Phys.* **4**, 32–36 (2008).
- Ryazanov, V. V., Oboznov, V. A., Veretennikov, A. V. & Rusanov, A. Y. Intrinsically frustrated superconducting array of superconductor–ferromagnet–superconductor  $\pi$  junctions. *Phys. Rev. B* **65**, 020501 (2001).
- Frolov, S. M., Van Harlingen, D. J., Oboznov, V. A., Bolginov, V. V. & Ryazanov, V. V. Measurement of the current–phase relation of superconductor/ferromagnet/superconductor  $\pi$  Josephson junctions. *Phys. Rev. B* **70**, 144505 (2004).
- Oboznov, V. A., Bolginov, V. V., Feofanov, A. K., Ryazanov, V. V. & Buzdin, A. I. Thickness dependence of the Josephson ground states of superconductor–ferromagnet–superconductor junctions. *Phys. Rev. Lett.* **96**, 197003 (2006).
- Likharev, K. K. & Semenov, V. K. RSFQ logic/memory family: A new Josephson-junction technology for sub-terahertz-clock-frequency digital systems. *IEEE Trans. Appl. Supercond.* **1**, 3–28 (1991).
- Ortlepp, T. *et al.* Flip-flopping fractional flux quanta. *Science* **312**, 1495–1497 (2006).
- Majer, J. B., Butcher, J. R. & Mooij, J. E. Simple phase bias for superconducting circuits. *Appl. Phys. Lett.* **80**, 3638–3640 (2002).
- Balashov, D. *et al.* Passive phase shifter for superconducting Josephson circuits. *IEEE Trans. Appl. Supercond.* **17**, 142–145 (2007).
- Mélin, R.  $\sin(2\varphi)$  current–phase relation in SFS junctions with decoherence in the ferromagnet. *Europhys. Lett.* **69**, 121–127 (2005).
- Hikino, S., Mori, M., Takahashi, S. & Maekawa, S. Ferromagnetic resonance induced Josephson current in a superconductor/ferromagnet/superconductor junction. *J. Phys. Soc. Jpn* **77**, 053707 (2008).
- Simmonds, R. W. *et al.* Decoherence in Josephson phase qubits from junction resonators. *Phys. Rev. Lett.* **93**, 077003 (2004).
- Chiorescu, I., Nakamura, Y., Harmans, C. J. P. M. & Mooij, J. E. Coherent quantum dynamics of a superconducting flux qubit. *Science* **299**, 1869–1871 (2003).
- Lisenfeld, J., Lukashenko, A., Ansmann, M., Martinis, J. M. & Ustinov, A. V. Temperature dependence of coherent oscillations in Josephson phase qubits. *Phys. Rev. Lett.* **99**, 170504 (2007).
- Kato, T., Golubov, A. A. & Nakamura, Y. Decoherence in a superconducting flux qubit with a  $\pi$ -junction. *Phys. Rev. B* **76**, 172502 (2007).
- Weides, M. *et al.*  $0-\pi$  Josephson tunnel junctions with ferromagnetic barrier. *Phys. Rev. Lett.* **97**, 247001 (2006).
- Bannykh, A. A. *et al.* Josephson tunnel junctions with a strong ferromagnetic interlayer. *Phys. Rev. B* **79**, 054501 (2009).
- Burmistrov, E. V. *et al.* A planar picoamperemeter based on a superconducting quantum interferometer. *J. Commun. Technol. Electr.* **51**, 1319–1324 (2006).

## Acknowledgements

This work was supported by the EU projects EuroSQIP and MIDAS. We acknowledge support by the Deutsche Forschungsgemeinschaft (DFG), the joint grant of DFG and Russian Foundation of Basic Research, the Russian Federal Agency of Science and Innovations, and the State of Baden–Württemberg through the DFG Center for Functional Nanostructures (CFN).

## Author contributions

A.K.F., V.A.O., V.V.R., A.B.Z. and A.V.U. contributed with ideas for the experiments. A.K.F., V.A.O., V.V.B., J.L., M.K., D.B. and V.P.K. designed samples. V.A.O., A.N.R., M.K., D.B. and P.N.D. fabricated samples. A.K.F., V.V.B., V.A.O., J.L., S.P., M.K. and D.B. carried out experiments and analysed the experimental data. A.K.F. made theoretical estimations. A.V.U., J.L., V.V.R. and A.B.Z. did most of the writing. All of the authors discussed the results and the manuscript extensively.

## Additional information

The authors declare no competing financial interests. Supplementary information accompanies this paper on [www.nature.com/naturephysics](http://www.nature.com/naturephysics). Reprints and permissions information is available online at <http://npg.nature.com/reprintsandpermissions>. Correspondence and requests for materials should be addressed to A.V.U.